

Lawrence Berkeley National Laboratory

LBL Publications

Title

CO₂ Absorption Process at the Liquid–Vapor Interface of Aqueous Monoethanol and Diethanol Amine Solutions

Permalink

<https://escholarship.org/uc/item/3hk224tn>

Journal

The Journal of Physical Chemistry C, 128(46)

ISSN

1932-7447

Authors

Siebert, Andreas

Goodman, Kenneth

Blum, Monika

Publication Date

2024-11-21

DOI

10.1021/acs.jpcc.4c06460

Peer reviewed

CO₂ Absorption Process at the Liquid–Vapor Interface of Aqueous Monoethanol and Diethanol Amine Solutions

Andreas Siebert, Kenneth Goodman, and Monika Blum*

Cite This: *J. Phys. Chem. C* 2024, 128, 19541–19549

Read Online

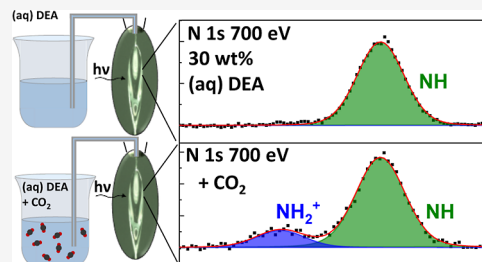
ACCESS |

Metrics & More

Article Recommendations

Supporting Information

ABSTRACT: CO₂ postcombustion is a promising technique to reduce the amount of CO₂ emissions from fossil fuel power plants. Aqueous amine solutions are among the most mature approaches to remove CO₂ from fume gases, but further efforts are required to overcome obstacles like the high amount of energy needed to strip the amine from the CO₂. A better understanding of the chemical reactions and the distribution of the reaction products in the crucial liquid–vapor interface region is of great importance for a deliberate improvement of the amine solutions. Ambient pressure X-ray photoelectron spectroscopy with a colliding micro liquid flat jet system was used to study 30 wt % aqueous monoethanolamine and diethanolamine solutions with different loading of CO₂. The observed concentrations of the different species in the bulk of our amine solution are in excellent agreement with infrared spectroscopy and nuclear magnetic resonance measurements from literature. Additionally, there is indication that the formed carbamate amine show a slight surface propensity, while the pure amine show a small tendency for the bulk of the solutions for both amine solutions at low CO₂ loadings.



INTRODUCTION

Climate change is already impacting large parts of humanity, and its devastating consequences are causing severe losses in life, well-being, and financial means.¹ One of its main causes is the emission of the greenhouse gas CO₂ into the earth's atmosphere.² The avoidance of CO₂ emissions is therefore of the highest priority, and where it is not feasible, the capturing and storage or utilization of CO₂ should be implemented.² Fossil fuel-operated power plants, for example, can be combined with a CO₂ postcombustion capturing (PCC) process to remove CO₂ from flue gas emitted by the power plant.³

One of the most mature CO₂ capturing processes is based on the chemical absorption of CO₂ using amine solvents, which offer fast absorption rates, high absorption capacities, and low material cost.^{4–6} In this process, flue gases are in a contactor exposed to an amine solution, which selectively reacts with the CO₂. In the second step, the amine will be heated, releasing the pure CO₂ for storage or utilization, while the regenerated amine solution is used in the next CO₂ absorption cycle. Lately, another CO₂ stripping procedure, utilizing CO₂ loaded aqueous amine solutions for the CO₂ curing of cement-based materials in construction, was suggested.⁷ Additionally, amines are not only limited to the PCC process but are also used in gas purification processes like selective H₂S absorption.⁸

Monoethanolamine (MEA) is a commonly studied primary amine that is already used in pilot power plants for CO₂ absorption.³ The major advantages of MEA over other amines include fast reaction kinetics and comparatively lower cost

associated.^{9,10} Diethanolamine (DEA) is a secondary amine, i.e., it has two organic substituents and only one hydrogen atom bound to nitrogen. Although the faster reaction kinetics and lower cost make MEA an attractive option, DEA has several advantages, i.e., lower reaction enthalpy and lower corrosiveness of the solution.⁹

For both MEA and DEA, the CO₂ absorption process mainly consists of the formation of a carbamate amine (amine-COO⁻) and a protonated amine (amine-H⁺) and can be described with the overall reaction¹¹



This limits the theoretical absorption capacity to 0.5 mol CO₂/mol amine; however, hydrogenation reactions of CO₂, like the formation of bicarbonates (HCO₃⁻) and carbonic acid (H₂CO₃) and CO₂ solvated in solution can lead to higher CO₂ absorption capacities.^{9,12}

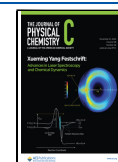
One of the main concerns hindering wider commercial implementation of the PCC is the high energy input required for CO₂ stripping, respectively, for amine regeneration. More than 2/3 of the energy cost of CO₂ capturing is related to the amine regeneration process.^{5,6} Additionally, the amine

Received: September 24, 2024

Revised: October 29, 2024

Accepted: November 1, 2024

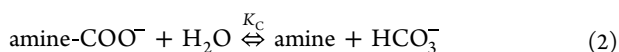
Published: November 8, 2024



decomposition due to side reactions can be a problem.⁶ Various amines and their blends have been investigated, and additionally, various catalytical approaches have been studied to decrease the energy penalty.^{5,6} However, a fundamental understanding of the involved reactions and their kinetics is often deficient, making current advancements dependent on a trial and error-based approach. For a deliberate improvement of the CO₂ capturing process, a detailed understanding of the complex chemistry at the liquid–vapor interface is required, as this is the main region where the chemical reactions occur. Studies of the amine–water–CO₂ system have been conducted among other techniques by nuclear magnetic resonance (NMR),^{9,12–14} Raman spectroscopy,¹⁵ infrared spectroscopy (IR),¹⁶ or titration.¹⁷ However, these techniques cannot provide information about the behavior at the interface, and theoretical modeling of the interface is costly, resulting in a relatively small number of publications focusing on the subject.^{18–21}

On the bulk end of the spectrum, the concentration of the formed species of the amine–water–CO₂-system can be predicted with a chemical model using experimentally observed chemical reaction equilibrium constants.^{9,15,16,22}

Therefore, the reaction equation for the formation of bicarbonate out of a carbamate amine is as follows



With the equilibrium constant K_C it can be used together with the nitrogen (amine) balance

$$[\text{amine}]_0 = [\text{amine}] + [\text{amine-H}^+] + [\text{amine-COO}^-] \quad (3)$$

the carbon CO₂ balance

$$\begin{aligned} [\text{CO}_2]_0 &= \alpha[\text{amine}]_0 \\ &= [\text{HCO}_3^-] + [\text{CO}_3^{2-}] + [\text{CO}_2] + [\text{amine-COO}^-] \end{aligned} \quad (4)$$

and the charge balance

$$\begin{aligned} [\text{H}_3\text{O}^+] + [\text{amine-H}^+] \\ &= [\text{HCO}_3^-] + 2[\text{CO}_3^{2-}] + [\text{OH}^-] + [\text{amine-COO}^-] \end{aligned} \quad (5)$$

In a simplified attempt from Du Preez et al., the eqs 4 and 5 can be facilitated with the following assumptions, which are shown to deliver good results for MEA.²² CO₂ reacts fully, leaving no CO₂ in solvation, and there are negligible hydroxide (OH⁻), hydronium (H₃O⁺) and carbonate (CO₃²⁻) ion concentrations for $\alpha < 0.6$ in equilibrium (α equals the molar CO₂ concentration per mol amine). This leads to

$$[\text{CO}_2]_0 = \alpha[\text{amine}]_0 = [\text{HCO}_3^-] + [\text{amine-COO}^-] \quad (6)$$

$$[\text{amine-H}^+] = [\text{HCO}_3^-] + [\text{amine-COO}^-] \quad (7)$$

Using eqs 2, 3, 6 and 7 together with the value of the equilibrium constant for eq 2, K_C , and the initial concentration of the amine ($[\text{amine}]_0$), the equation system can be solved for different values of α and the equilibrium concentrations of carbamate amine, protonated amine, free amine, and bicarbonate can be determined for the bulk solution.

An excellent technique, providing insights into the crucial interface region of a system, is ambient pressure X-ray photoelectron spectroscopy (APXPS), where differential

pumping stages are separating the ultra-high vacuum conditions of the detector from the ambient pressure conditions (up to a few Torr) in the experimental chamber. APXPS is a very surface sensitive method (information depth up to a few nanometers) due to the short effective attenuation length (EAL) of the excited electrons. It allows to differentiate elements and chemical species due to the chemical shift, making it one of the few techniques capable of providing information about the chemical composition at a surface or interface.²³ Furthermore, the probing depth depends on the electron kinetic energy, enabling information depth profiling with an energy tunable photon source.²³ In recent years, the liquid–vapor interface became accessible for APXPS among others due to the usage of liquid jet systems.^{18,23–26} A special liquid jet setups is the colliding liquid flat jet setup, providing the ability to study the mixing of different solutions.²⁴ Nevertheless, the flat surface has additional advantages over the more common circular jet systems such as a more suitable sample geometry. The average subsurface probing depth of a planar surface of a flat jet is enhanced by a factor of $\pi/2$ compared to the cylindrical surface of a circular jet (for a 90° incident beam compared to the electron detector direction), resulting in a better signal-to-noise ratio and enabling measurements of low concentrated solutions.^{23,26}

In this paper, our colliding micro liquid flat jet system was used in the LARaXS endstation, described in detail elsewhere,²⁷ at beamline 11.0.2.1 of the Advanced Light Source (ALS),²⁸ to study the liquid–vapor interface of aqueous MEA and DEA solutions at different levels of CO₂ loading with APXPS. We compared our obtained concentrations of CO₂ absorption reaction products with results from literature for the bulk concentration^{16,22} and furthermore highlighted the differences between the concentrations in the near surface and bulk region of the amine solutions, providing the first step to a better understanding of the chemical processes at the interface enabling a deliberate manufacturing of better amine-based solvents.

EXPERIMENTAL SECTION

Aqueous MEA (Sigma-Aldrich, ACS reagent, ≥99.0%) and DEA (Sigma-Aldrich, ACS reagent, ≥99.0%) solutions with 30 wt % have been produced by mixing pure amine solutions with deionized water. The initial pH values were 12.40 for MEA and 11.67 for DEA (12.54 and 11.53 in literature).¹² Afterward, CO₂ (Airgas, 99.9%) at different concentrations was bubbled into the aqueous amine solutions in an open container at a pressure of 1 atm, while monitoring the change of the pH value and the mass increase, which was used to calculate the respective concentration of mol CO₂ per mol amine, see Table 1. Solutions with the same pH value have been prepared twice, and the presented values correspond to the average mass increase, while the uncertainty is half of the difference between the two measurements. After no further CO₂ uptake was observed, the MEA solution had a pH value of 8.52 and a CO₂ uptake of 0.51 mol/mol MEA. PH measurements were performed using a VWR pH 1100 H pH meter with a VWR pHenomenal 111 pH electrode calibrated by three VWR International technical buffer solutions having a pH of 4.01, 7.00, and 10.00 at 25 °C.

The APXPS measurements were performed at beamline 11.0.2.1 of the ALS²⁷ in the LARaXS endstation using a colliding micro liquid flat jet system described elsewhere.²⁷

Table 1. Overview Over the Measured Solutions and Their Corresponding pH Values

MEA 30 wt % aqueous solution	pH	mmol CO ₂ /mol MEA	DEA 30 wt % aqueous solution	pH	mmol CO ₂ /mol DEA
MEA	12.40	0	DEA	11.67	0
MEA 1st CO ₂ loading	11.94	13 ± 8	DEA 1st CO ₂ loading	11.15	17 ± 3
MEA 2nd CO ₂ loading	11.47	35 ± 16	DEA 2nd CO ₂ loading	10.80	38 ± 12
MEA 3rd CO ₂ loading	8.52	509 ± 1	DEA 3rd CO ₂ loading	10.47	62 ± 8
			DEA 4th CO ₂ loading	9.88	162 ± 2

The used jet nozzles had an aperture diameter of 35 μm (for the aqueous 30 wt % MEA and DEA solution) and 30 μm (for all solutions with a CO₂ loading), and the Knauer Blue Shadow 40P HPLC pump was operated with pressures around 65 bar and flow rates of 4 mL/min (35 μm nozzle apertures) and 3.2 mL/min (30 μm nozzle apertures), to form a liquid flat sheet. Together with a liquid nitrogen filled cooling trap, the pressure in the experimental chamber was in the low 10⁻⁴ Torr region during all measurements.

Since both the N 1s and C 1s core levels contain information about the amount of amine (sum of both peak areas in the N 1s core level and the CH₂ peak in the C 1s core level), all peak areas can be normalized relative to the total amount of amine. Assuming that the total amount of amine in the measurement region is always similar to the initial amount of amine present in the prepared aqueous solutions, i.e., 4.9 M for MEA and 2.9 M for DEA, the concentrations of the different amine species have been calculated. With this approach, a correction of the experimental raw data for the analyzer transmission function, the photon flux, the respective cross section for each core level, and the electron attenuation length is not required.

In the Supporting Information, Figure S3, we show an updated version of Figure 4, with uncertainties for the concentrations derived from assuming a difference in the overall amine concentration of 6% in the bulk and surface. It can be seen that this uncertainty is negligible compared to the uncertainty derived from the fit for small concentrations like the measured carbamate and protonated amine concentrations at low CO₂ loading. However, for higher concentrations like the free amine concentrations, a potential difference in the overall amine concentration could have a large impact. A difference of 6% was chosen, as this is the largest difference in the concentrations of a species between the surface and bulk that we have measured in a solution (carbamate concentration of the DEA third CO₂ loading solution). Anyways, a potential difference in the overall amine concentration can have an influence on the absolute species concentration observed in the surface and bulk region, but the relative amount will always stay the same; i.e., there are, for example, more carbamate amines in the surface region with respect to the overall amine concentration compared to the bulk region at low CO₂ loadings.

Peak areas have been derived from core level fits with Voigt functions and a linear background function using the program fityk 0.9.3.²⁹ The binding energies of the C 1s spectra were adjusted so that the CH₂ peaks are at the literature value of 291 eV, and the binding energies of the N 1s spectra have been adjusted so that the NH/NH₂ peaks match the literature value

of 406.4 eV.¹⁸ Information regarding the Lorentzian and Gaussian FWHM can be found in the Supporting Information.

RESULTS

30 wt % aqueous solutions of MEA and DEA have been prepared with different CO₂ loadings, and the APXPS C 1s and N 1s core level have been measured with the colliding liquid flat jet system. Electron kinetic energies of 300 and 700 eV were obtained, exploiting the energy tunability of the synchrotron light. In Figure 1 the measured C 1s spectra are shown for all amine solutions, showing the more interface sensitive 300 eV electron kinetic energy measurements on the left and the more bulk sensitive 700 eV measurements on the right. The electron kinetic energy of 300 and 700 eV correspond to an information depth, i.e., electron EAL of roughly 2 and 5 nm (assuming a pure water solution as an estimate).²⁶

The pH values and the CO₂ loading per mol of amine are shown for every spectrum. The MEA pH value of 8.52 for the 0.51 CO₂/mol MEA saturated solution is comparable to literature results of 8.5 and 8.4.^{18,19} However, lower pH values have been reported related to higher CO₂ loadings. Below a pH of 8.5, the hydration of CO₂ and the formation of bicarbonates (HCO₃⁻) and/or carbonic acid (H₂CO₃) become the main reaction responsible for the CO₂ uptake.¹²

All spectra were fitted with a maximum of two Voigt functions and a linear background function. The main (green) peak was assigned to CH₂ groups of the amine, present in the free and reacted amine, and the peak area can always be related to the total amount of amine present in the investigated region of the solution. A second (blue) peak with a 2.5 eV higher binding energy, similarly observed in the literature,¹⁸ corresponds to COO⁻ carbamate species (MEA-COO⁻ and DEA-COO⁻) formed between amine and CO₂ following reaction 1. It is clearly visible that the COO⁻ species rises with the increased CO₂ loading for MEA and DEA.

In contrast to the previous liquid jet APXPS measurements on a CO₂ saturated MEA solution with a pH value of 8.4, no carbamic acid (COOH) has been observed.¹⁸ Nevertheless, this is in agreement with NMR measurements performed on aqueous MEA and DEA solutions with different CO₂ loadings.^{12,14} Those measurements showed the formation of bicarbonate or carbonic acid usually starting at higher CO₂ loadings, i.e., pH values below 8.5. Hence, a significant contribution of these species is not expected for our investigated amine solutions with relatively high pH values and low CO₂ loadings. Only the 0.51 mol CO₂/mol MEA solution with a measured pH value of 8.52 might contain an additional bicarbonate species superposed with the MEA-COO⁻ peak, see Figure S1 and the related discussion in the Supporting Information.

The much higher equilibrium vapor pressure of water 2.35 kPa compared to the amine at 20 °C (for MEA \approx 35 Pa and for DEA <1 Pa) leads to a much higher formation of water vapor compared to amine vapor (<1%) in the experimental chamber and explains that no gas phase amine species have been observed in the XPS spectra.^{30–33} Similar to the literature results, we cannot differentiate between the protonated and neutral amine in the C 1s spectra; however, this is possible in the N 1s core level spectra presented in Figure 2.¹⁸

Here, the spectra have been again fitted with a maximum of 2 Voigt functions and a linear background function. The green main peak was related to the free amine NH₂-group of MEA,

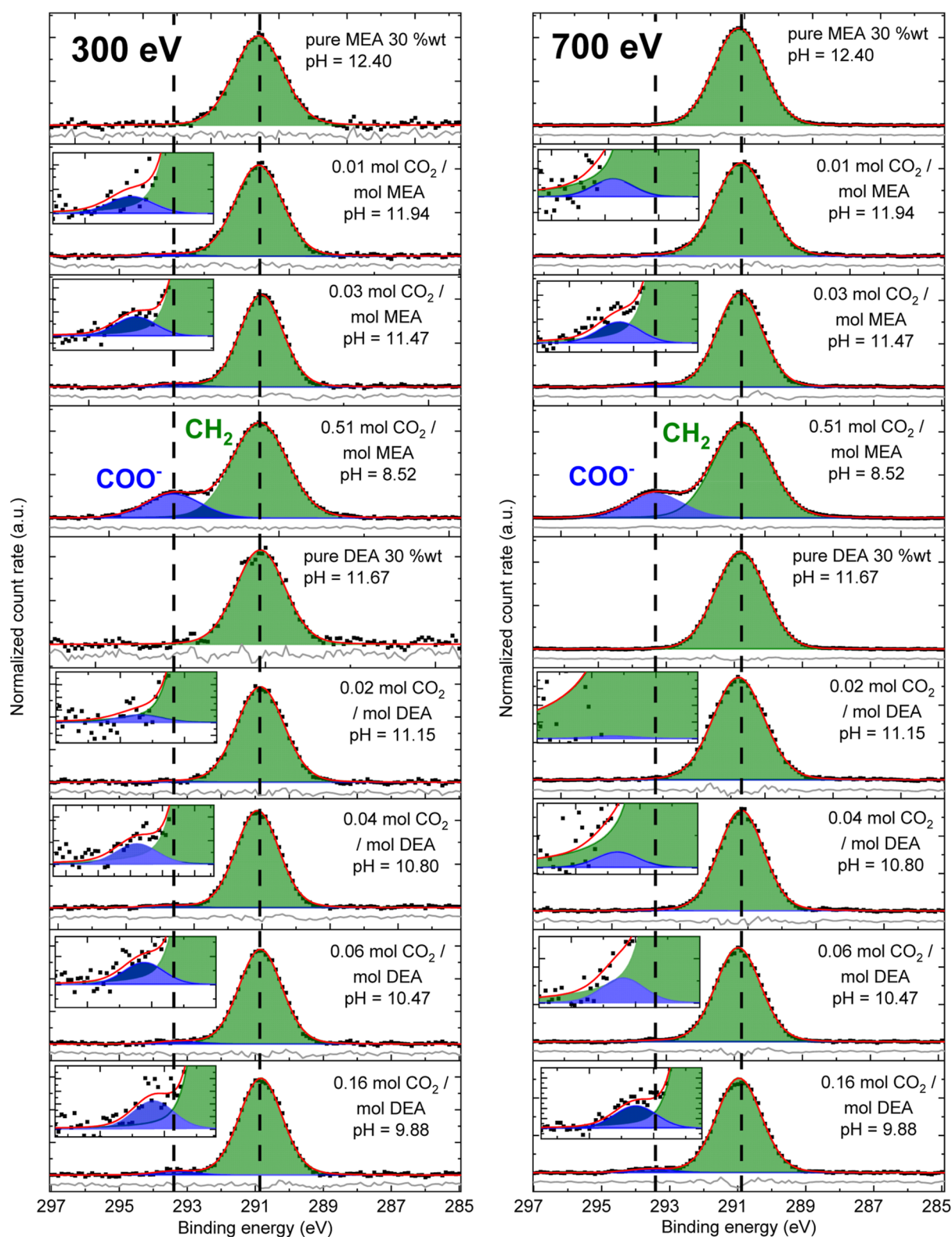


Figure 1. C 1s core levels of MEA and DEA with increasing CO₂ loading measured with 300 eV (left) and 700 eV (right) electron kinetic energy using excitation energies of 585 eV and 985 eV. The green peak corresponds to the CH₂ group, and the blue peak corresponds to the carbamate COO⁻ group. When necessary, insets zoomed in on the blue peak are provided to increase the visibility.

respectively, the NH-group of DEA. With increasing CO₂ loading, an additional blue peak arises with an average 2.3 eV higher binding energy (2.4 eV in literature)¹⁸ that was related to the protonated amine NH₃⁺ of MEA (MEA-H⁺) and NH₂⁺ of DEA (DEA-H⁺). The nitrogen group of the carbamate

amine species cannot be differentiated from the nitrogen group of the free amine (NH/NH₂). The sum of the blue and green peak areas can be related to the total amount of amine present in the measurement region of the solution. With the C 1s and N 1s spectra, all reaction products during the CO₂ absorption

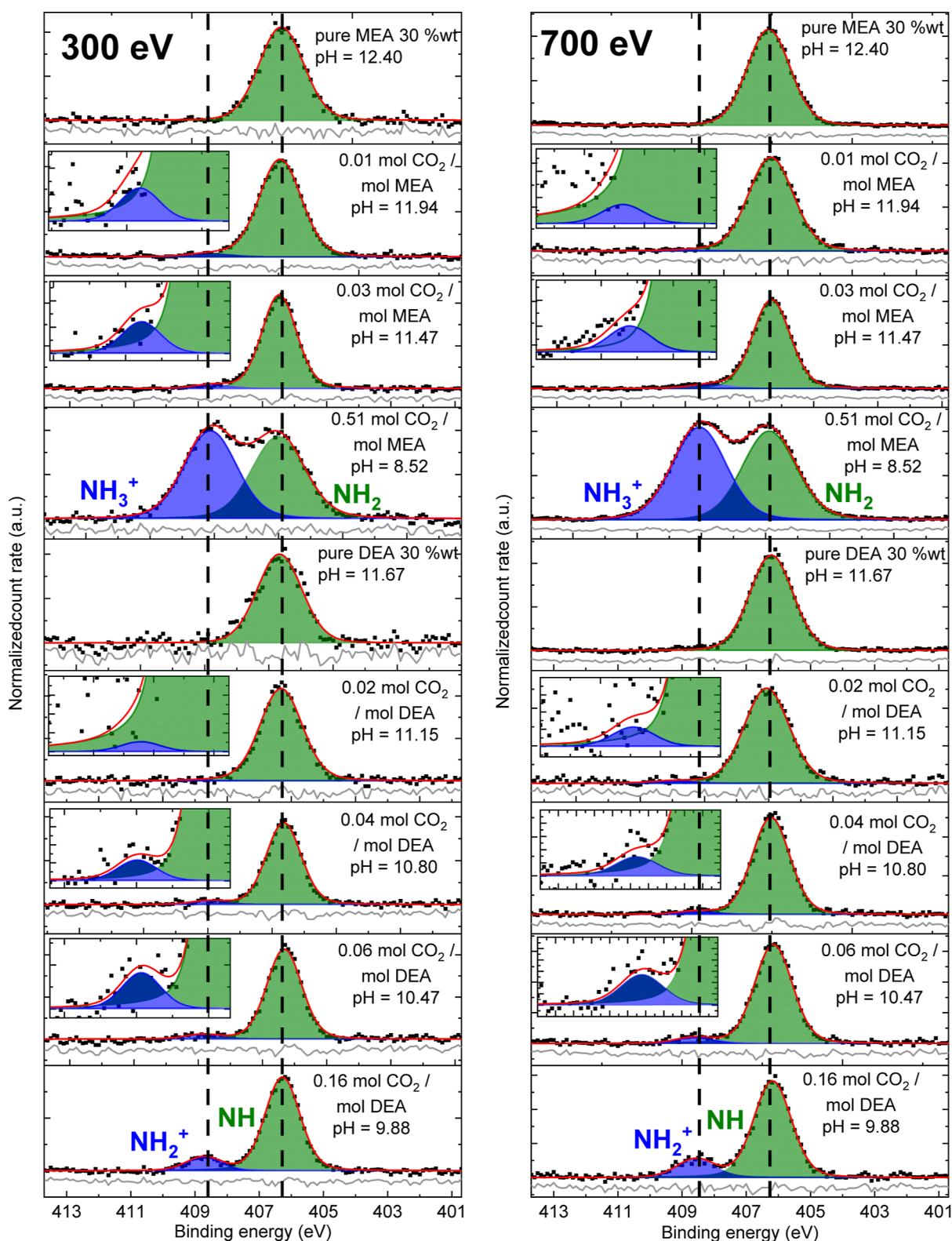


Figure 2. N 1s core levels of MEA and DEA with increasing CO₂ loading measured with 300 eV (left) and 700 eV (right) electron kinetic energy using excitation energies of 700 eV and 1100 eV. The green peak corresponds to neutral nitrogen NH/NH₂, and the blue peak corresponds to protonated amine NH₂⁺/NH₃⁺. When necessary, insets zoomed in on the blue peak are provided to increase the visibility.

process, i.e., protonated and carbamate amine, can be identified and related to the total amount of amine present in that region of the solution, avoiding a peak area correction for effective electron attenuation length, analyzer transmission

function, and the core level cross sections, which are not necessarily well-defined/studied for liquids.²⁶

Obtained from the more bulk sensitive measurements, the concentration (mol/L) of the free amine (MEA and DEA), protonated amine (MEA-H⁺ and DEA-H⁺), and carbamate

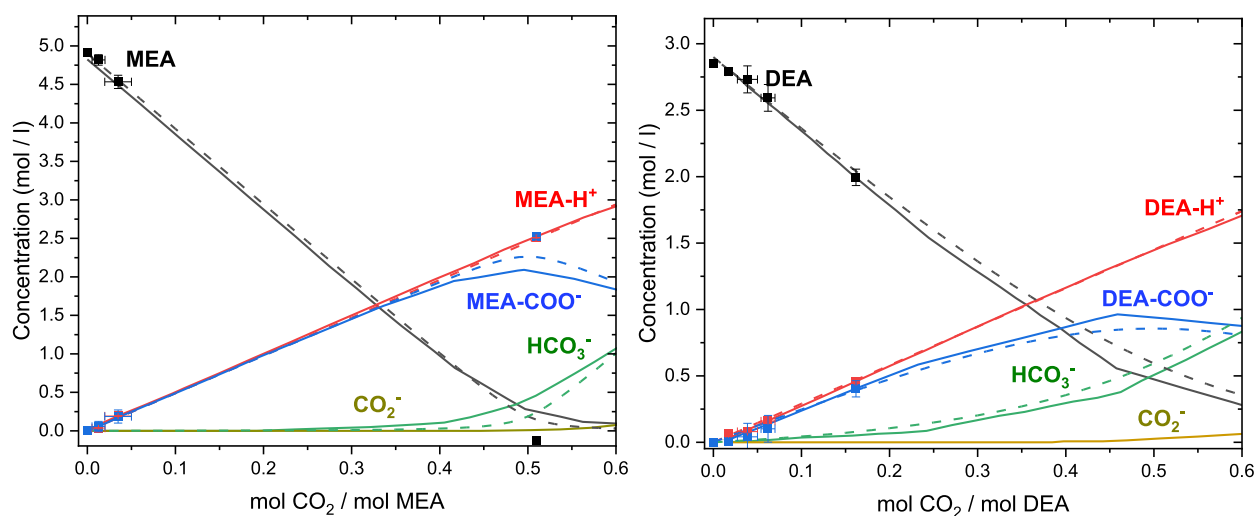


Figure 3. Concentration (mol/L) of free amine (MEA and DEA), protonated amine (MEA-H⁺ and DEA-H⁺), and carbamate amine (MEA-COO⁻ and DEA-COO⁻) are shown with respect to the CO₂ loading per mol amine for MEA on the left side and DEA on the right side. The results are compared with bulk sensitive IR measurements from Richner et al. (solid lines) and a simplified VLE model from the literature based on NMR measurements of Böttinger et al. (dashed lines).^{16,22} Reproduced from [16]. Copyright [2012] American Chemical Society and [22]. Copyright [2018] American Chemical Society.

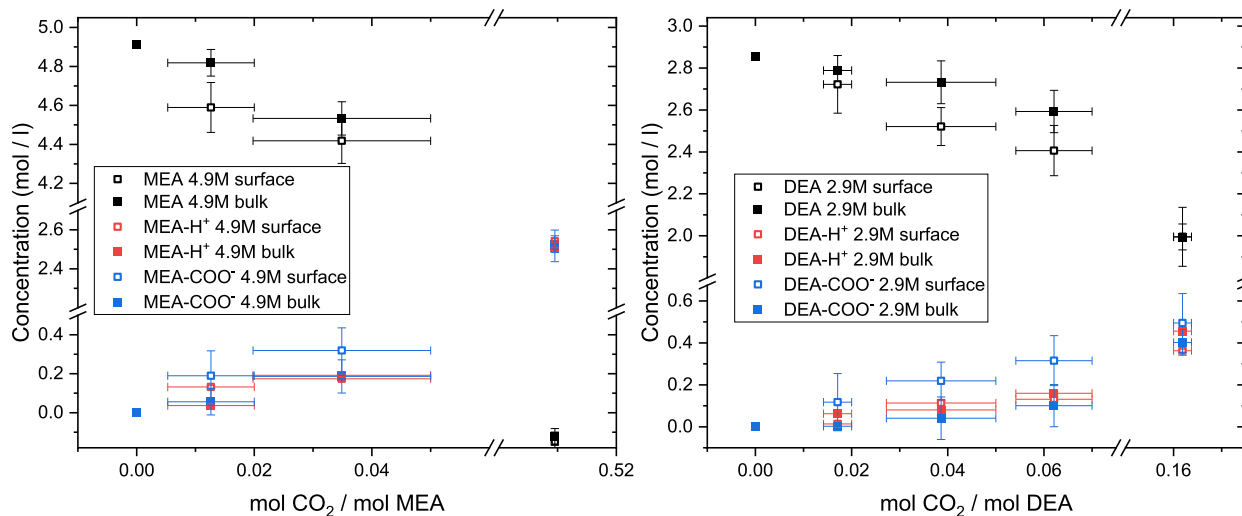


Figure 4. Concentrations (mol/L) of the free amine (MEA and DEA), protonated amine (MEA-H⁺ and DEA-H⁺), and carbamate amine (MEA-COO⁻ and DEA-COO⁻) are shown with respect to the CO₂ loading per mol amine for MEA on the left side and DEA on the right side. The concentrations have been measured with an electron kinetic energy of 300 eV (open squares), related to the more surface sensitive and 700 eV (solid squares), related to the more bulk sensitive measurements.

amine (MEA-COO⁻ and DEA-COO⁻) is shown in Figure 3 over the respective CO₂ loading per mol amine for MEA on the left side and DEA on the right side. The error bars of the concentrations correspond to the uncertainties derived from the standard error of the fit of each spectrum provided by Fityk.

The results are compared with IR measurements reported by Richner et al. from the literature similarly conducted on aqueous amine solutions with a 30 wt % amine loading. Additionally, shown in Figure 3 are calculated amine concentrations from a simplified vapor–liquid–equilibrium model similar to the literature²² using the eqs 2, 3, 6 and 7, assuming 30 wt % amine solutions and the equilibrium constants obtained with NMR measurements for MEA and DEA by Böttinger et al.⁹

$$\ln K_{C,MEA} = \left(\frac{-3255.31}{T} + 6.6203 + \frac{4.564T}{10^4} \right) = \frac{[\text{HCO}_3^-][\text{MEA}]}{[\text{MEA-COO}^-]} \quad (8)$$

$$\ln K_{C,DEA} = \left(\frac{-3173.21}{T} + 14.9018 - \frac{172.42T}{10^4} \right) = \frac{[\text{HCO}_3^-][\text{DEA}]}{[\text{DEA-COO}^-]} \quad (9)$$

with a temperature of $T = 298$ K. Calculations using other experimentally determined values for the equilibrium constants from the literature, for example, for MEA at $T = 298$ K²² and for DEA at $T = 298$ K³⁴ and at $T = 313.15$ K¹⁵ show only very small deviations compared to the presented curves in Figure 3.

In general, the calculations using the vapor–liquid–equilibrium model are in excellent agreement with our measurements and the IR results at low CO₂ loadings.¹⁶ For example, the same splitting between protonated and carbamate amines for DEA and to a lesser extent for MEA is present in all results of Figure 3.

The biggest difference between our measurements and the literature results is the absence of dissolved bicarbonates HCO₃[−] and CO₂[−] in our measurements. However, the expected amount of CO₂[−] solved in the solution is generally small. Furthermore, the solutions in literature^{9,15,16,22} have been prepared in closed containers at higher pressures, which favors the solubility of CO₂.⁹ Nevertheless, the concentrations of the free MEA and carbamate MEA for the 0.51 mol CO₂/mol MEA solution show the biggest discrepancies with respect to the concentrations observed in the literature and even an unphysical, slightly negative value for the free MEA concentration. This supports the already mentioned theory that there is an additional HCO₃[−] species present in the C 1s spectra superposed with the MEA-COO[−] peak for the 0.51 mol CO₂/mol MEA solution. This results in an overestimation of the MEA carbamate amount and an underestimation in the free MEA and HCO₃[−] species, see Figure S2 and the related discussion in the Supporting Information.

Figure 4 shows the differences of the concentrations of the observed amine species between the more surface sensitive 300 eV and the more bulk sensitive 700 eV electron kinetic energy measurements for MEA on the left side and DEA on the right side. Again, the error bars of the concentrations correspond to the uncertainties derived from the standard error of the fits. In general, the differences between the concentrations are small, and the error bars are often overlapping. There are some slight differences visible especially for the low CO₂ loadings, most prominent, the concentrations of carbamate MEA and carbamate DEA seem to be larger at the surface compared to the bulk. On the other hand, the free MEA and free DEA concentrations seem to be larger in the bulk at low CO₂ loadings, while there is no clear trend observable for the protonated MEA and protonated DEA. The concentrations of the 0.51 mol CO₂/mol MEA solution show no preference toward the surface or the bulk.

To the authors knowledge, the only other published APXPS investigation of amine solutions (aqueous 4.9 M MEA) was done by Lewis et al.¹⁸ This work suggests a larger concentration of free MEA at the surface and more protonated and carbamate MEA in the bulk, which is somewhat contrary to the indication in our data. However, there are several reasons that could explain this difference. First of all, Lewis et al. measured only one CO₂ treated solution, with a pH value of 8.4 and a CO₂ loading of 0.24 mol CO₂/mol MEA, showing a large difference in CO₂ loading compared to our and literature solutions with a similar pH value.^{18,19}

Our MEA solution with a close pH value of 8.52 eV does not show significant differences between the concentrations and does not show the trends we see for low CO₂ loadings for MEA and DEA solutions. Another important difference are the selected kinetic energies, of 90 and 590 eV, which are more surface sensitive compared to the kinetic energies used here.

If our observed differences in the surface and bulk concentrations are significant and if they have a relevant impact on the CO₂ reaction kinetics, further investigations would be warranted. One may speculate that a bulk propensity of the free amine hinders faster CO₂ absorption kinetics,

assuming that the reaction mainly occurs at the liquid–vapor interface. On the other hand, a surface propensity of the carbamate amine might favor the release reaction of CO₂. This suggests it might be possible to increase reaction kinetics by finding a solution with an enhanced surface concentration of free CO₂ sorbent or alternatively find additives to promote the concentration at the surface, potentially a good addition or alternative to an increased liquid–gas interface area in the contactor.³⁵

However, the observed differences in the concentrations are small, and the impact on the reaction kinetics, if any, so far is unclear and beyond the scope of this work. A conclusive APXPS depth profile exploiting smaller electron kinetic energy steps could reveal additional details of the aqueous amine systems and may allow for better differentiation between the bicarbonate and carbamate amine contributions to the investigated solutions.

CONCLUSIONS

We have conducted for the first time APXPS measurements on 30 wt % aqueous MEA and DEA solutions with different CO₂ loadings using a colliding micro flat jet system. Exploiting electron kinetic energies of 300 and 700 eV, we studied the differences in the concentration of the formed species close to the liquid–vapor interface and deeper in the bulk of the solution. Our results indicate a bulk propensity for the free amine and a surface propensity for the carbamate amine at low CO₂ loadings for both amine solutions, while the protonated amine concentration is roughly the same between the more surface and more bulk sensitive measurements. The observed concentrations of the bulk sensitive measurements show an excellent agreement with literature results.^{9,16} In contrast to previous APXPS measurements of a CO₂ saturated aqueous MEA solution, we have not observed a formation of carbamic acid.¹⁸ Our results demonstrate the power of liquid flat jet systems and emphasize the crucial role of the liquid–vapor interface in the CO₂ absorbance of aqueous MEA and DEA solutions, paving the way to a deliberate development or improvement of CO₂ sorbents in the future.

ASSOCIATED CONTENT

Supporting Information

The Supporting Information is available free of charge at <https://pubs.acs.org/doi/10.1021/acs.jpcc.4c06460>.

Included is a potential HCO₃[−] contribution in the 0.51 mol CO₂/mol MEA solution overlapping in the C 1s spectrum with the COO[−] contribution, and the corresponding concentrations of the newly calculated MEA-COO[−] and the free MEA. Furthermore the impact of a potential difference in the overall amine concentration and details regarding the N1s and C1s fits are presented (PDF)

AUTHOR INFORMATION

Corresponding Author

Monika Blum – Advanced Light Source, Lawrence Berkeley National Laboratory, Berkeley, California 94720, United States; Chemical Sciences Division, Lawrence Berkeley National Laboratory, Berkeley, California 94720, United States; orcid.org/0000-0002-2918-9092; Email: mblum@lbl.gov

Authors

Andreas Siebert – Advanced Light Source, Lawrence Berkeley National Laboratory, Berkeley, California 94720, United States; Chemical Sciences Division, Lawrence Berkeley National Laboratory, Berkeley, California 94720, United States

Kenneth Goodman – Chemical Sciences Division, Lawrence Berkeley National Laboratory, Berkeley, California 94720, United States; orcid.org/0000-0003-2656-1685

Complete contact information is available at:
<https://pubs.acs.org/10.1021/acs.jpcc.4c06460>

Notes

The authors declare no competing financial interest.

ACKNOWLEDGMENTS

This research used resources of the Advanced Light Source, which is a DOE Office of Science User Facility under contract no. DE-AC02-05CH11231. All authors were supported by the Condensed Phase and Interfacial Molecular Science Program in the Chemical Sciences Geosciences and Biosciences Division of the Office of Basic Energy Sciences of the U.S. Department of Energy under contract no. DE-AC02-05CH11231. The authors are thankful for Stephan Figul from Advanced Microfluidic Systems GmbH for his technical support.

REFERENCES

- (1) Newman, R.; Noy, I. The Global Costs of Extreme Weather That Are Attributable to Climate Change. *Nat. Commun.* **2023**, *14* (1), 6103.
- (2) Calvin, K.; Dasgupta, D.; Krinner, G.; Mukherji, A.; Thorne, P. W.; Trisos, C.; Romero, J.; Aldunce, P.; Barrett, K.; Blanco, G.; et al. IPCC, 2023: Climate Change 2023: Synthesis Report. In *Contribution of Working Groups I, II and III to the Sixth Assessment Report of the Intergovernmental Panel on Climate Change [Core Writing Team; Lee, H., Romero, J., Eds.; IPCC, Intergovernmental Panel on Climate Change (IPCC): Geneva, Switzerland, 2023*.
- (3) Deiana, P.; Bassano, C.; Cali, G.; Miraglia, P.; Maggio, E. CO₂ Capture and Amine Solvent Regeneration in Sotacarbo Pilot Plant. *Fuel* **2017**, *207*, 663–670.
- (4) Dutcher, B.; Fan, M.; Russell, A. G. Amine-Based CO₂ Capture Technology Development from the Beginning of 2013—A Review. *ACS Appl. Mater. Interfaces* **2015**, *7* (4), 2137–2148.
- (5) Waseem, M.; Al-Marzouqi, M.; Ghasem, N. A Review of Catalytically Enhanced CO₂-Rich Amine Solutions Regeneration. *J. Environ. Chem. Eng.* **2023**, *11* (4), 110188.
- (6) Zhang, X.; Zhang, R.; Liu, H.; Gao, H.; Liang, Z. Evaluating CO₂ Desorption Performance in CO₂-Loaded Aqueous Tri-Solvent Blend Amines with and without Solid Acid Catalysts. *Appl. Energy* **2018**, *218*, 417–429.
- (7) Han, S. H.; Jun, Y.; Kim, J. H. The Use of Monoethanolamine CO₂ Solvent for the CO₂ Curing of Cement-Based Materials. *Sustainable Mater. Technol.* **2023**, *35*, No. e00559.
- (8) Lu, J.-G.; Zheng, Y.-F.; He, D.-L. Selective Absorption of H₂S from Gas Mixtures into Aqueous Solutions of Blended Amines of Methyl-diethanolamine and 2-Tertiarybutylamino-2-Ethoxyethanol in a Packed Column. *Sep. Purif. Technol.* **2006**, *52* (2), 209–217.
- (9) Böttinger, W.; Maiwald, M.; Hasse, H. Online NMR Spectroscopic Study of Species Distribution in MEA–H₂O–CO₂ and DEA–H₂O–CO₂. *Fluid Phase Equilib.* **2008**, *263* (2), 131–143.
- (10) Heldebrant, D. J.; Koeck, P. K.; Glezakou, V.-A.; Rousseau, R.; Malhotra, D.; Cantu, D. C. Water-Lean Solvents for Post-Combustion CO₂ Capture: Fundamentals, Uncertainties, Opportunities, and Outlook. *Chem. Rev.* **2017**, *117* (14), 9594–9624.
- (11) Abotaleb, A.; Gladich, I.; Alkhateeb, A.; Mardini, N.; Bicer, Y.; Sinopoli, A. Chemical and Physical Systems for Sour Gas Removal: An Overview from Reaction Mechanisms to Industrial Implications. *J. Nat. Gas Sci. Eng.* **2022**, *106*, 104755.
- (12) Lv, B.; Guo, B.; Zhou, Z.; Jing, G. Mechanisms of CO₂ Capture into Monoethanolamine Solution with Different CO₂ Loading during the Absorption/Desorption Processes. *Environ. Sci. Technol.* **2015**, *49* (17), 10728–10735.
- (13) Fan, G.; Wee, A. G. H.; Idem, R.; Tontiwachwuthikul, P. NMR Studies of Amine Species in MEA–CO₂–H₂O System: Modification of the Model of Vapor–Liquid Equilibrium (VLE). *Ind. Eng. Chem. Res.* **2009**, *48* (5), 2717–2720.
- (14) Liu, H.; Li, M.; Luo, X.; Liang, Z.; Idem, R.; Tontiwachwuthikul, P. Investigation Mechanism of DEA as an Activator on Aqueous MEA Solution for Postcombustion CO₂ Capture. *AIChE J.* **2018**, *64* (7), 2515–2525.
- (15) Souchon, V.; Aleixo, M. D. O.; Delpoux, O.; Sagnard, C.; Mougou, P.; Wender, A.; Raynal, L. In Situ Determination of Species Distribution in Alkanolamine–H₂O–CO₂ Systems by Raman Spectroscopy. *Energy Procedia* **2011**, *4*, 554–561.
- (16) Richner, G.; Puxty, G. Assessing the Chemical Speciation during CO₂ Absorption by Aqueous Amines Using in Situ FTIR. *Ind. Eng. Chem. Res.* **2012**, *51* (44), 14317–14324.
- (17) Matin, N. S.; Remias, J. E.; Neathery, J. K.; Liu, K. Facile Method for Determination of Amine Speciation in CO₂ Capture Solutions. *Ind. Eng. Chem. Res.* **2012**, *51* (19), 6613–6618.
- (18) Lewis, T.; Faubel, M.; Winter, B.; Hemminger, J. C. CO₂ Capture in Amine-Based Aqueous Solution: Role of the Gas–Solution Interface. *Angew. Chem., Int. Ed.* **2011**, *50* (43), 10178–10181.
- (19) McWilliams, L. E.; Valley, N. A.; Vincent, N. M.; Richmond, G. L. Interfacial Insights into a Carbon Capture System: CO₂ Uptake to an Aqueous Monoethanolamine Surface. *J. Phys. Chem. A* **2017**, *121* (41), 7956–7967.
- (20) Huang, I.-S.; Li, J.-J.; Tsai, M.-K. Solvation Dynamics of CO₂(g) by Monoethanolamine at the Gas–Liquid Interface: A Molecular Mechanics Approach. *Molecules* **2016**, *22* (1), 8.
- (21) Sinopoli, A.; Abotaleb, A.; Pietrucci, F.; Gladich, I. Stability of a Monoethanolamine–CO₂ Zwitterion at the Vapor/Liquid Water Interface: Implications for Low Partial Pressure Carbon Capture Technologies. *J. Phys. Chem. B* **2021**, *125* (18), 4890–4897.
- (22) Du Preez, L. J.; Motang, N.; Callanan, L. H.; Burger, A. J. Determining the Liquid Phase Equilibrium Speciation of the CO₂–MEA–H₂O System Using a Simplified in Situ Fourier Transform Infrared Method. *Ind. Eng. Chem. Res.* **2019**, *58* (1), 469–478.
- (23) Dupuy, R.; Richter, C.; Winter, B.; Meijer, G.; Schlögl, R.; Bluhm, H. Core Level Photoelectron Spectroscopy of Heterogeneous Reactions at Liquid–Vapor Interfaces: Current Status, Challenges, and Prospects. *J. Chem. Phys.* **2021**, *154* (6), 060901.
- (24) Stemer, D.; Buttersack, T.; Haak, H.; Malerz, S.; Schewe, H. C.; Trinter, F.; Mudryk, K.; Pugini, M.; Credidio, B.; Seidel, R.; Hergenhan, U.; Meijer, G.; Thürmer, S.; Winter, B. Photoelectron Spectroscopy from a Liquid Flatjet. *J. Chem. Phys.* **2023**, *158* (23), 234202.
- (25) Chang, Y.-P.; Yin, Z.; Balciunas, T.; Wörner, H. J.; Wolf, J.-P. Temperature Measurements of Liquid Flat Jets in Vacuum. *Struct. Dynam.* **2022**, *9* (1), 014901.
- (26) Ottosson, N.; Faubel, M.; Bradforth, S. E.; Jungwirth, P.; Winter, B. Photoelectron Spectroscopy of Liquid Water and Aqueous Solution: Electron Effective Attenuation Lengths and Emission-Angle Anisotropy. *J. Electron Spectrosc. Relat. Phenom.* **2010**, *177* (2–3), 60–70.
- (27) Siebert, A.; Goodman, K.; Figul, S.; Blum, M. Technical Manuscript Flat Jet. **2023**. DOI: .
- (28) Bluhm, H.; Andersson, K.; Araki, T.; Benzerara, K.; Brown, G. E.; Dynes, J. J.; Ghosal, S.; Gilles, M. K.; Hansen, H.-Ch.; Hemminger, J. C.; et al. Soft X-Ray Microscopy and Spectroscopy at the Molecular Environmental Science Beamline at the Advanced Light Source. *J. Electron Spectrosc. Relat. Phenom.* **2006**, *150* (2–3), 86–104.

- (29) Wojdyr, M. Fityk: a general-purpose peak fitting program. *J. Appl. Crystallogr.* **2010**, *43* (5), 1126–1128.
- (30) Kim, I.; Svendsen, H. F.; Borresen, E. Ebulliometric Determination of Vapor–Liquid Equilibria for Pure Water, Monoethanolamine, N-Methyldiethanolamine, 3-(Methylamino)-Propylamine, and Their Binary and Ternary Solutions. *J. Chem. Eng. Data* **2008**, *53* (11), 2521–2531.
- (31) *Perry's Chemical Engineers' Handbook*, 7th ed.; Perry, R. H., Green, D. W., Maloney, J. O., Eds.; McGraw-Hill: New York, 1997, PP 97.
- (32) Wilding, W. V.; Knotts, T. A.; Giles, N. F.; Rowley, R. L. DIPPR Data Compilation of Pure Chemical Properties. *Des. Inst. Phys. Prop. AIChE*, **2020**.
- (33) Klepáčová, K.; Huttenhuis, P. J. G.; Derks, P. W. J.; Versteeg, G. F. Vapor Pressures of Several Commercially Used Alkanolamines. *J. Chem. Eng. Data* **2011**, *56* (5), 2242–2248.
- (34) Aroua, M. K.; Amor, A. B.; Haji-Sulaiman, M. Z. Temperature Dependency of the Equilibrium Constant for the Formation of Carbamate From Diethanolamine. *J. Chem. Eng. Data* **1997**, *42* (4), 692–696.
- (35) Gruenewald, M.; Radnjanski, A. Gas–Liquid Contactors in Liquid Absorbent-Based PCC. In *Absorption-Based Post-Combustion Capture of Carbon Dioxide*; Elsevier, 2016; pp 341–363.